Evidence of soft modes in magnetoelectric $CuFeO_2$: Ultrasonic velocity measurements and Landau theory

G. Quirion, M. J. Tagore, and M. L. Plumer
Department of Physics and Physical Oceanography, Memorial University, St. John's, Newfoundland, Canada A1B 3X7

O. A. Petrenko
Department of Physics, University of Warwick, Coventry CV4 7AL, United Kingdom
(Received 3 October 2007; published 11 March 2008)

Ultrasonic velocity measurements are used to examine the elastic properties of the magnetoelectric compound $CuFeO_2$ in the vicinity of the magnetic and structural phase transitions near 14 K. Strong softening of modes related to C_{66} occurs at the transition from the high-temperature rhombohedral $R\bar{3}m$ to lower-temperature monoclinic $C2/m$ symmetry. A Landau free energy is proposed and analyzed in order to understand the elastic properties of $CuFeO_2$. The principal features of sound velocity modes vs temperature are reproduced by the model. Our analysis suggests that the transition at 14 K is primary *pseudoproper ferroelastic*, with the spin acting as a secondary order parameter.

DOI: 10.1103/PhysRevB.77.094111 PACS number(s): 64.60.−i, 62.20.D−, 75.80.+q, 75.50.Ee

I. INTRODUCTION

Frustrated spin systems, caused by competing interactions or lattice geometries such as in triangular-lattice antiferromagnet, continue to attract considerable attention due to their exotic magnetic characteristics. This interest is principally owed to frustration, which leads to a large number of nearly degenerate spin configurations that potentially order at low temperatures. In particular, there has been a renewed interest in multiferroic compounds and the magnetoelectric effect. This exotic effect, where a moderate magnetic field induces an electrical polarization, has been recently observed in compounds such as $TbMnO_3$,[1] $Ni_3V_2O_8$,[2] and $CuFeO_2$.[3] Due to the interplay between magnetism, ferroelectricity, and structural deformations, understanding these systems represents a serious challenge.[4]

As with many of the more popular magnetoelectric hexagonal $RMnO_3$ compounds,[5] the magnetic transition metal ions in $CuFeO_2$ form stacked triangular layers within the high-temperature crystal structure, which is rhombohedral $R\bar{3}m$ in the present case. In zero magnetic field, the Fe^{3+} ions order into an incommensurate linearly polarized spin structure (with $\mathbf{S}\|\hat{\mathbf{c}}$) below $T_{N1}\simeq 14$ K. With further decrease in temperature, the incommensurate spin configuration suddenly changes (first-order transition) into a period-4 basal-plane modulated commensurate order at $T_{N2}\simeq 11$ K, again with $\mathbf{S}\|\hat{\mathbf{c}}$.[6] The application of a magnetic field along the c axis produces a rich phase diagram[3,7] and stabilizes a noncollinear spin structure between 7 and 12 T, which, by coupling through the intersite lattice vector $\mathbf{r}_{ij}=\mathbf{r}_i-\mathbf{r}_j$, induces an electric polarization $\mathbf{P}\sim\mathbf{r}_{ij}\times(\mathbf{S}_i\times\mathbf{S}_j)$.[3,8]

In the temperature regime between 14 and 11 K, neutron and x-ray diffraction measurements[9,10] have revealed a structural transition from the high-temperature ($T>14$ K) rhombohedral symmetry $R\bar{3}m$ to a low-temperature ($T<11$ K) monoclinic $C2/m$ phase. This transformation is induced by an elongation of the hexagonal basal-plane lattice constant b_H along with a concomitant contraction of c_H. The detailed nature of the crystal structure in the intermediate region is unclear,[10] and it has been suggested that an incommensurate modulation of the lattice sites occurs.[9] The strong pressure dependence of T_{N1} and T_{N2} (Refs. 11 and 12) along with x-ray diffraction measurements,[13,14] showing magnetic-field-induced lattice distortions, provide clear evidence for significant magnetoelastic coupling in $CuFeO_2$. Further investigation into the interplay between magnetic, elastic, and electric properties in geometrically frustrated antiferromagnets is essential for a complete understanding of a large class of magnetoelectric materials.

In the present work, a detailed investigation of the structural phase transition in $CuFeO_2$ is made through high resolution ultrasonic velocity measurements over a temperature range from 4 to 50 K. This technique has proven useful in the characterization of related transitions in a variety of systems.[15–17] The present results reveal a nearly complete softening of modes associated with the elastic constant C_{66} at about 14 K and clear anomalies in other modes at this temperature, as well as at a lower temperature close to 11 K. These temperatures are coincident with the magnetic phase transitions. For convenience, both magnetic and structural transition temperatures will be labeled T_{N1} and T_{N2}. The results clearly establish the important role of the elastic properties in understanding the exotic magnetic and magnetoelectric behaviors of $CuFeO_2$.

The analysis of a Landau model free energy, based on symmetry arguments, shows good agreement with the temperature dependence of the measured velocity modes as well as the previously reported pressure dependence of T_{N1}. Application of this model leads to the conclusion that the structural transition at 14 K is primarily *pseudoproper ferroelastic*,[18] with the spin acting as a secondary order parameter. A brief discussion on the role of spin-lattice coupling within the framework of the Landau model is presented in this paper.

The remainder of the paper is organized as follows. We briefly describe the experimental methods in Sec. II, while the experimental results are presented in Sec. III. In order to interpret those results, an appropriate Landau model is de-

TABLE I. Expression of ρv^2 for the trigonal and monoclinic phases. Note that solutions for the monoclinic phase are obtained using a coordinate system with the twofold symmetry axis parallel to $\hat{\mathbf{x}}$. For that reason, expressions given here differ from the conventional setting with the twofold axis along $\hat{\mathbf{z}}$. The symbol $\sim$ is used to indicate that the polarization is close to the direction listed.

Acoustic modes Direction/Polarization		Trigonal $R\bar{3}m$ phase	Monoclinic $C2/m$ phase
[100]	L^* [100]	C_{11}	C_{11}
	$T_1{}^* \sim$[010]	$\frac{1}{2}(C_{44}+C_{66}-\sqrt{(C_{44}-C_{66})^2+4C_{14}^2})$	$\frac{1}{2}(C_{55}+C_{66}+\sqrt{(C_{55}-C_{66})^2+4C_{56}^2})$
	$T_2 \sim$[001]	$\frac{1}{2}(C_{44}+C_{66}+\sqrt{(C_{44}-C_{66})^2+4C_{14}^2})$	$\frac{1}{2}(C_{55}+C_{66}-\sqrt{(C_{55}-C_{66})^2+4C_{56}^2})$
[010]	L [010]	$\frac{1}{2}(C_{11}+C_{44}+\sqrt{(C_{11}-C_{44})^2+4C_{14}^2})$	$\frac{1}{2}(C_{22}+C_{44}+\sqrt{(C_{22}-C_{44})^2+4C_{24}^2})$
	$T_1{}^*$[100]	C_{66}	C_{66}
	T_2 [001]	$\frac{1}{2}(C_{11}+C_{44}-\sqrt{(C_{11}-C_{44})^2+4C_{14}^2})$	$\frac{1}{2}(C_{22}+C_{44}-\sqrt{(C_{22}-C_{44})^2+4C_{24}^2})$
[001]	L^* [001]	C_{33}	$\frac{1}{2}(C_{33}+C_{44}+\sqrt{(C_{33}-C_{44})^2+4C_{34}^2})$
	$T_1{}^*$[100]	C_{44}	C_{55}
	T_2 [010]	C_{44}	$\frac{1}{2}(C_{33}+C_{44}-\sqrt{(C_{33}-C_{44})^2+4C_{34}^2})$

rived in Sec. IV along with the principal predictions for the variation of the elastic properties associated with an $R\bar{3}m \rightarrow C2/m$ pseudoproper ferroelastic phase transition. A comparison between the model and experimental results is presented in Sec. V. A final discussion and conclusion is made in Sec. VI.

II. EXPERIMENT

The ultrasound velocity experiments were performed on single crystals of $CuFeO_2$ grown using an infrared image furnace.[7] Several samples were prepared with polished parallel faces normal to the principal crystallographic directions. All samples were roughly cubic in shape with edges of approximately 3 mm in length. For this investigation, longitudinal or transverse waves were generated and detected using 30 MHz $LiNbO_3$ transducers bonded on opposite faces of the samples. Measurements were made using a pulsed acoustic interferometer, which allows for the detection of a relative variation in velocity $(\Delta v/v)$ as small as 1 ppm.

III. ELASTIC PROPERTIES AND EXPERIMENTAL RESULTS

At room temperature, $CuFeO_2$ belongs to the rhombohedral space group $R\bar{3}m$, for which the elastic tensor consists of six independent components.[19] These constants are linked to the velocity v of acoustic modes propagating along a direction $\vec{q}$ through the eigenvalues of the Chritoffel equation.[19] The principal modes for ρv^2, with ρ representing the mass density, are listed in Table I for the $R\bar{3}m$ rhombohedral and $C2/m$ monoclinic groups. Both sets of expressions are obtained using a unique coordinate system defined relative to the high-temperature rhombohedral structure (threefold symmetry axis along $\hat{\mathbf{z}}$ with a twofold symmetry axis along $\hat{\mathbf{x}}$). Our expressions for the monoclinic structure differ from those found in most text books[19] where, by convention, the twofold symmetry axis is oriented along $\hat{\mathbf{z}}$. As shown in Table I, the principal elastic constants of $CuFeO_2$ can be obtained by measuring the velocity of two longitudinal (L) and three transverse (T) modes identified by an asterisk.

The measured temperature dependence from 4 to 50 K of the relative variation of the velocity $\Delta v/v$ corresponding to these five modes is presented in Fig. 1. All velocity curves have been normalized relative to the maximum value observed around 100 K. Except for transverse modes presented in Fig. 1(a), for which no signal was observed below T_{N1}, all modes show two distinct anomalies at 13.7 and 10.6 K. These temperatures coincide very well with the zero-field magnetic phase transition temperatures observed previously in specific heat,[7] magnetization,[7] x-ray,[9,10] and neutron diffraction[7,20] experiments. No significant hysteresis was detected at T_{N1}, while a discontinuity in the velocity accompanied by a thermal hysteresis of $\Delta T=0.5$ K is observed at T_{N2}, confirming the first-order character of this transition.

The most striking feature in the results presented in Fig. 1 is the decrease in the velocity of all modes measured as the temperature approaches T_{N1}. This is particularly evident in the velocity of transverse modes propagating along x or y with a polarization (P) also into the basal plane [Fig. 1(a)]. According to Table I, a 30% decrease in $V_{T_y}(P_x)$ (0.3 K above T_{N1}) represents a 50% reduction of C_{66} relative to its value at 100 K. Due to large acoustic attenuation, we were unable to obtain data below, or just above, T_{N1}. For that reason, we have no direct experimental evidence that the mode associated with $V_{T_x}(P_y)$ shows complete softening at T_{N1}. This observation alone would have clearly indicated that the nature of the transition at T_{N1} is ferroelastic.[21] Whereas the softening on C_{66} is considerable, Figs. 1(c) and 1(d) indicate that the softening on C_{44} $[V_{T_z}(P_x)]$ and C_{33} (V_{L_z}) is at least 2 orders of magnitude smaller. Finally, we note that the softening on C_{11} is significant, as V_{L_x} [Fig. 1(b)] shows a decrease of 6.5% at T_{N1}.

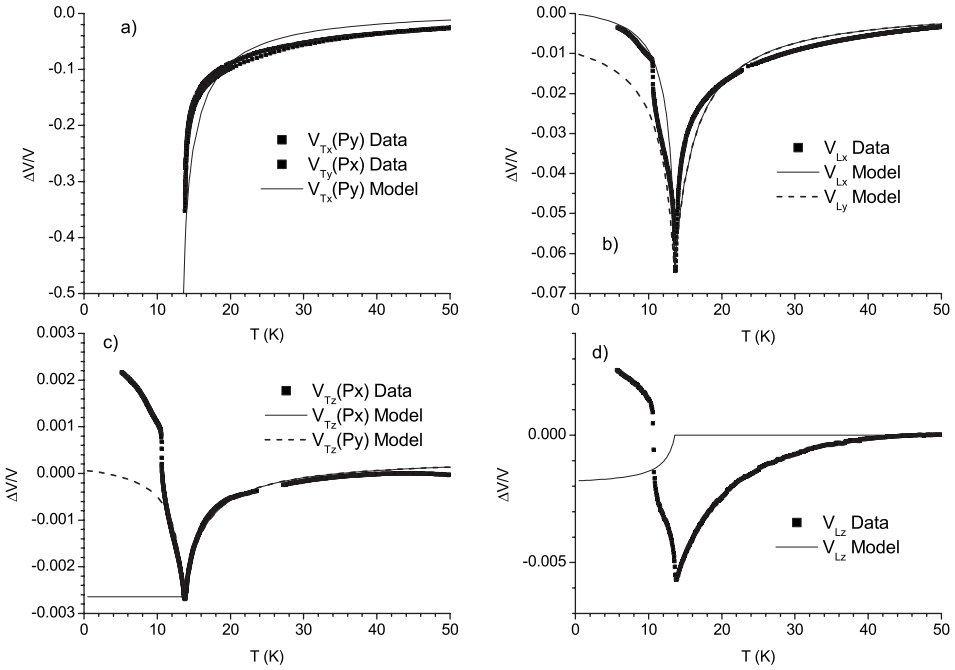

FIG. 1. Temperature dependence of the relative velocity variation. The direction of propagation of longitudinal (L) and transverse (T) modes is indicated by the label index, while the polarization, whenever required, appears between the parentheses. Experimental data are represented by symbols, while solid lines are used for predictions derived from the model presented in Sec. IV. Note the large differences in vertical scales between the graphs.

IV. LANDAU MODEL OF THE ELASTIC PROPERTIES

Since the transverse acoustic mode propagating in the xy plane shows considerable softening close to T_{N1}, it is natural to assume that the main character of that structural phase transition is ferroelastic. In this case, two scenarios need to be examined depending on the nature of the order parameter Q.[21,22] If the order parameter is one of the strain components e_s (or combination of strains), the transition is referred to as a proper-ferroelastic transition. In this case, which appears to be extremely rare, the temperature and pressure dependence of the effective elastic constant associated with soft acoustic mode is linear over a wide range.[16,23] This feature is not consistent with our data. Elastic softening can also be attributed to a so-called pseudoproper ferroelastic transition. In such a case, the order parameter Q and the strain e_s belong to the same irreducible representation so that a bilinear coupling term such as e_sQ is allowed. In this case, the pressure or temperature dependence of the acoustic soft mode is generally nonlinear as in KH_2PO_4,[24] where the order parameter (the z component of the electric polarization P_z) couples to the shear acoustic mode e_6, resulting in the softening of C_{66}. Similar softening is also evident in other compounds such as $BiVO_4$,[25] LaP_5O_14,[26] and SnO_2,[27] where the order parameter is associated with a soft optical mode. Thus, according to the experimental results presented in this work, it is reasonable to assume that the character of the structural phase transition in $CuFeO_2$ at T_{N1} is pseudoproper ferroelastic.

This assumption can be tested by comparing the predictions from a pseudoproper type Landau free energy to the elastic properties of $CuFeO_2$ in the paraelastic phase and close to T_{N1}. According to the 64 species of ferroelastic transitions,[18] only two possible phase sequences, $R\bar{3}m \rightarrow \bar{1}$ and $R\bar{3}m \rightarrow C2/m$, need to be considered. However, as recent x-ray diffraction data[9,10] indicate that Bragg reflections corresponding to $R\bar{3}m$ and monoclinic symmetries coexist below T_{N1}, we believe that the latter scenario is more likely. The fact that $R\bar{3}m$ reflection peaks persist in the monoclinic phase can be attributed to structural domains which always exist in ferroelastic materials.[28] We present in this section a pseudoproper ferroelastic Landau-type model, derived from symmetry principles, to account for the elastic properties of $CuFeO_2$. Knowing that the transition at T_{N1} satisfies the group-subgroup symmetry criteria, the order parameter Q must belong to the two-dimensional irreducible representation E (x^2-y^2,xy) of the $R\bar{3}m$ space group.[29] As none of the spin components belong to this representation, the observed softening in $CuFeO_2$ must be attributed to a different order parameter Q. Possible coupling between spin degrees of freedom S and Q is discussed in Sec. V.

As tabulated by Tolédano *et al.*,[21] the Landau free energy of an $R\bar{3}m \rightarrow C2/m$ ferroelastic compound can be expressed as a function of a two component order parameter $\{Q_1,Q_2\}$

$$F_L(Q_i) = \frac{1}{2}A(Q_1^2+Q_2^2) + \frac{1}{4}B(Q_1^2+Q_2^2)^2 + \frac{1}{3}C(Q_1^3-3Q_1Q_2^2), \tag{1}$$

where $A=a(T-T_0)$ and $B>0$. Here, T_0 defines the transition temperature in the absence of elastic coupling [see Eq. (8) below]. In principle, as odd power terms are allowed, the transition should be discontinuous. To our knowledge, only two trigonal ferroelastic compounds have been modeled by this free energy. After much controversy over whether the transitions were continuous or first order, results on s-triazine[30] $C_3H_3N_3$ and sodium azide[16,31] NaN_3 have now been confirmed to exhibit small discontinuities. Thus, in principle, the structural transition at T_{N1} in $CuFeO_2$ could also be weakly first order. However, there is presently no experimental evidence supporting that possibility. In order to

simplify the present analysis, only the first two terms of Eq. (1) are considered here.

In order to calculate the elastic properties, additional contributions such as elastic deformations, as well as coupling terms between these deformations and the order parameter, need to be considered in the model. The form of the elastic energy $F_{el}(e_\alpha)$ is dictated by the symmetry of the $R\bar{3}m$ phase[19] and is given by

$$F_{el}(e_\alpha) = \frac{1}{2}C_{11}(e_1^2+e_2^2) + \frac{1}{2}C_{33}e_3^2 + \frac{1}{2}C_{44}(e_4^2+e_5^2) + \frac{1}{2}C_{66}e_6^2 + C_{12}e_1e_2 + C_{13}(e_1+e_2)e_3 + C_{14}(e_1-e_2)e_4 + C_{14}e_5e_6, \quad (2)$$

with $C_{66}=(C_{11}-C_{12})/2$. Here, the elastic constants $C_{\alpha\beta}$ and strains e_α are expressed using the Voigt notation[19] (α, $\beta=1-6$). For a pseudoproper ferroelastic transition, the order parameter Q and the spontaneous strain e_s must belong to the same irreducible representation and the allowed coupling terms have been identified by imposing that $Q=\{Q_1,Q_2\}$ transform as the strain combinations $e_s=\delta_1\{e_1-e_2,e_6\}+\delta_2\{e_4,e_5\}$.[21] Under these considerations, the lower-order coupling terms allowed by symmetry are limited to

$$F_c(Q_i,e_\alpha) = \delta_1[(e_1-e_2)Q_1+e_6Q_2] + \delta_2(e_4Q_1+e_5Q_2) + \beta_1(e_1+e_2)(Q_1^2+Q_2^2) + \beta_3e_3(Q_1^2+Q_2^2). \quad (3)$$

A contribution associated with hydrostatic pressure P

$$F_P(P,e_\alpha) = (e_1+e_2+e_3)P \quad (4)$$

is also considered. This is particularly convenient as it can be used to calculate dT_{N1}/dP.

Minimization of the Gibbs energy

$$G(Q_i,e_\alpha) = F_L + F_{el} + F_c + F_P \quad (5)$$

with respect to e_α leads to solutions, in terms of the order parameter components and pressure, corresponding to

$$e_1-e_2 = \frac{2(\delta_2C_{14}-\delta_1C_{44})}{C_a}Q_1,$$

$$e_1+e_2 = \frac{2(\beta_3C_{13}-\beta_1C_{33})}{C_b}(Q_1^2+Q_2^2) - \frac{C_e}{C_b}P,$$

$$e_3 = -\frac{\beta_3(C_{11}+C_{12})-2\beta_1C_{13}}{C_b}(Q_1^2+Q_2^2) - \frac{C_d}{C_b}P,$$

$$e_4 = \frac{(-\delta_2(C_{11}-C_{12})+2\delta_1C_{14})}{C_a}Q_1,$$

$$e_5 = \frac{(-\delta_1C_{14}+\delta_2C_{66})}{C_c}Q_2,$$

$$e_6 = \frac{(-\delta_2C_{14}+\delta_1C_{44})}{C_c}Q_2, \quad (6)$$

with

$$C_a = (C_{11}-C_{12})C_{44} - 2C_{14}^2,$$

$$C_b = (C_{11}+C_{12})C_{33} - 2C_{13}^2,$$

$$C_c = C_{14}^2 - C_{44}C_{66},$$

$$C_d = C_{11}+C_{12}-2C_{13},$$

$$C_e = 2(C_{33}-C_{13}). \quad (7)$$

Minimization with respect to Q_i results into three possible stable phases corresponding to the usual high-temperature paraelastic phase ($Q_1=Q_2=0$), a solution with ($Q_1\neq 0$, $Q_2=0$) which preserves the twofold symmetry ($C2/m$ phase), and a state characterized by ($Q_1\neq 0$, $Q_2\neq 0$) corresponding to a $\bar{1}$ triclinic phase. Thus, according to these solutions, an $R\bar{3}m\rightarrow C2/m$ ferroelastic phase transition at T_{N_1} should be described by $Q_2=0$ and be accompanied by spontaneous strain components e_1, e_2, e_3, and e_4, while $e_5=e_6=0$. These predictions are supported by x-ray diffraction measurements,[10] which show large spontaneous strains for $\Delta b_M=e_2$ and $\Delta a_H=(e_1+e_2)/2$, while there is no experimental data reported for e_4. We also find that the temperature dependence of e_1-e_2 and e_4 follows that of Q_1, given by

$$Q_1(T) \approx \sqrt{\frac{a\left(T_{N1}-T+\frac{dT_{N1}}{dP}P\right)}{2B}},$$

$$T_{N1} = T_0 - \frac{C_f}{2aC_a},$$

$$\frac{dT_{N1}}{dP} = \frac{\beta_3C_d+\beta_1C_e}{aC_b}, \quad (8)$$

with $C_f=\delta_2^2(C_{11}-C_{12})+2\delta_1(\delta_1C_{44}-2\delta_2C_{14})$. As we can see, the effect of the bilinear coupling term between Q and e is to shift the transition temperature from its uncoupled limit of T_0 to T_{N1}.

Solutions for the elastic constants are obtained from the total free energy using[32]

$$C_{mn}^* = \frac{\partial^2F}{\partial e_m\partial e_n} - \sum_i \frac{\partial^2F}{\partial Q_i\partial e_m}\left(\frac{\partial^2F}{\partial Q_i^2}\right)^{-1}\frac{\partial^2F}{\partial e_n\partial Q_i}. \quad (9)$$

Results of these calculations, as a function of $A(T)$ and the order parameter $Q(T)$ at ambient pressure, are tabulated in Table II. According to this model, five of seven independent elastic constants in the trigonal phase should show softening depending on the values of the coupling coefficients δ_1 and δ_2. The model also gives 13 independent elastic constants at low temperature, which is compatible with the monoclinic phase.[19] It is important to note that the nonzero elements obtained here, for the monoclinic structure, differ from those reported in most references[19] as a more convenient coordinate system is used. For the present calculation, the free

TABLE II. Temperature dependence of the elastic constants for an $R\bar{3}m \rightarrow C2/m$ pseudoferroelastic phase transition.

	Trigonal $R\bar{3}m$	Monoclinic $C2/m$
C_{11}	$C_{11}^{\circ}-\frac{\delta_1^2}{A(T)}$	$C_{11}^{\circ}-\frac{(\delta_1+2\beta_1 Q_1)^2}{A(T_c)+2BQ_1^2}$
C_{22}	$C_{11}^{\circ}-\frac{\delta_1^2}{A(T)}$	$C_{11}^{\circ}-\frac{(\delta_1-2\beta_1 Q_1)^2}{A(T_c)+2BQ_1^2}$
C_{33}	C_{33}°	$C_{33}^{\circ}-\frac{4\beta_3^2 Q^2}{A(T_c)+2BQ_1^2}$
C_{44}	$C_{44}^{\circ}-\frac{\delta_2^2}{A(T)}$	$C_{44}^{\circ}-\frac{\delta_2^2}{A(T_c)+2BQ_1^2}$
C_{55}	$C_{44}^{\circ}-\frac{\delta_2^2}{A(T)}$	$C_{44}^{\circ}-\frac{\delta_2^2}{A(T_c)}$
C_{66}	$C_{66}^{\circ}-\frac{\delta_1^2}{A(T)}$	$C_{66}^{\circ}-\frac{\delta_1^2}{A(T_c)}$
C_{12}	$C_{12}^{\circ}+\frac{\delta_1^2}{A(T)}$	$C_{12}^{\circ}+\frac{\delta_1^2-4\beta_1^2 Q_1^2}{A(T_c)+2BQ_1^2}$
C_{13}	C_{13}°	$C_{13}^{\circ}-\frac{(\delta_1+2\beta_1 Q_1)2\beta_3 Q_1}{A(T_c)+2BQ_1^2}$
C_{14}	$C_{14}^{\circ}-\frac{\delta_1\delta_2}{A(T)}$	$C_{14}^{\circ}-\frac{(\delta_1+2\beta_1 Q_1)\delta_2}{A(T_c)+2BQ_1^2}$
C_{23}	C_{13}°	$C_{13}^{\circ}+\frac{(\delta_1-2\beta_1 Q_1)2\beta_3 Q_1}{A(T_c)+2BQ_1^2}$
C_{24}	$-C_{14}^{\circ}+\frac{\delta_1\delta_2}{A(T)}$	$-C_{14}^{\circ}+\frac{(\delta_1-2\beta_1 Q_1)\delta_2}{A(T_c)+2BQ_1^2}$
C_{34}	0	$-\frac{2\beta_3 Q_1\delta_2}{A(T_c)+2BQ_1^2}$
C_{56}	$C_{14}^{\circ}-\frac{\delta_1\delta_2}{A(T)}$	$C_{14}^{\circ}-\frac{\delta_1\delta_2}{A(T_c)}$

energy is defined relative to the high-temperature phase using the conventional coordinate system for the elastic tensor associated with the $R\bar{3}m$ trigonal phase. Consequently, the threefold axis is parallel to the z axis, while the twofold axis is along the x axis. As the $R\bar{3}m \rightarrow C2/m$ phase transition must preserve the twofold symmetry, the calculated elastic tensor for the monoclinic structure conserves the twofold symmetry along the x direction. This configuration differs from the conventional setting, where the twofold symmetry coincides with the z axis of the monoclinic structure.

V. NUMERICAL PREDICTIONS AND DISCUSSION

All constants included in this model have been determined using specific experimental observations. Values of the bare elastic constants, except for C_{13}° and C_{14}°, reported in Table III have been determined from absolute sound velocity measurements taken at 100 K. The remaining constants have been estimated by comparing relevant model equations with experimental observations, such as velocity measurements (this work), the pressure dependence of T_{N1},[11] and lattice constants as a function of temperature[10] and pressure.[33] These relations correspond to

$$\frac{1}{2}\frac{\Delta C_{11}(T_{N_1})}{C_{11}^{\circ}} = -6.5\ \%\ ,$$

$$\frac{1}{2}\frac{\Delta C_{11}(16K)}{C_{11}^{\circ}} = -3.5\ \%\ ,$$

$$\frac{1}{2}\frac{\Delta C_{44}(T_{N_1})}{C_{44}^{\circ}} = -0.3\ \%\ ,$$

$$\frac{e_1(P)+e_2(P)}{e_3(P)} = 7.6,$$

$$e_1(Q_0)-e_2(Q_0) = -0.01,$$

$$e_1(Q_0)+e_2(Q_0) = 0.0001,$$

$$dT_{N1}/dP = -1\ \text{K/GPa}, \tag{10}$$

where $Q_0=Q_1(T=0\ \text{K})$ as given by Eq. (8). The coupling constants derived from these solutions are listed in Table IV. The calculated temperature dependence of the acoustic modes are compared to the experimental results and presented in Fig. 1. Considering that some coupling constants are determined using experimental data independent of this work, the agreement between calculated and experimental velocities is more than satisfactory. As for NaN_3,[16,34] which shows an $R\bar{3}m \rightarrow C2/m$ proper-ferroelastic transition, the soft acoustic mode associated with the spontaneous strain e_s is given by

$$C_s = \frac{1}{2}(C_{44}+C_{66}-\sqrt{(C_{44}-C_{66})^2+4C_{14}^2}), \tag{11}$$

which turns out to be equivalent to the effective elastic constant of the transverse mode propagating along the x axis (T_1 mode in Table III). According to our calculation, the polarization of the soft mode should be in the yz plane at an angle of 16° relative to the y axis. If the transition is, indeed, continuous, the velocity of this mode should drop to zero at T_{N1}; otherwise, as in the case of NaN_3,[16,31] a small but finite velocity could be measured by Brillouin scattering measurements. The softening on C_{66} is also predicted to be large, with a reduction of 98% at T_{N1} relative to its value at 100 K. These predictions could not be tested using our acoustic sys-

TABLE III. Experimental values of the bare elastic constants at 100 K.

Bare values	C_{11}°	C_{12}°	C_{13}°	C_{14}°	C_{33}°	C_{44}°	C_{66}°
10^{10} N/m^2	15(1)	11(1)	11(1)	0.28(4)	24(2)	1.1(1)	1.9(1)

TABLE IV. Values of the coupling constants.

a	B	T_0	δ_1	δ_2	β_1	β_3
1	2.11×10^{-5}	10.7	2.38×10^{5}	1.36×10^{4}	−60	−100

tem as the signal disappears close to T_{N1} due to a rapid increase in the acoustic attenuation.

The model can also be used in order to predict the temperature dependence of the velocities in the low-temperature phase. As shown in Fig. 1(b), calculations for longitudinal modes propagating along the x and y directions indicate that the velocity along these directions should be quite different in the low-temperature phase. The same observation applies to transverse waves propagating along the z axis with a polarization parallel to the x or y direction [see Fig. 1(c)]. Additional measurements have been made in order to detect the velocity anisotropy in the low-temperature phase; however, no significant differences have been observed. We attribute the lack of anisotropy at low temperatures to structural domains that are known to exist in ferroelastic materials.[28] Due to these domains, the acoustic measurements, which probe the macroscopic properties, reveal an effective trigonal symmetry even at low temperatures. This is supported by x-ray diffraction measurements[10] which show that Bragg reflections corresponding to trigonal symmetry do persist below T_{N1}.

Finally, consider the temperature dependence of V_{L_z}, which indicates softening on the value of C_{33} [Fig. 1(d)]. As shown thus far, the proposed model accounts for the softening of all other modes also presented in the same figure. However, for C_{33}, the experimental observation is inconsistent with the model's prediction. As a linear-linear coupling term such as e_3Q is strictly forbidden under inversion operation, the ferroelastic model cannot account for the softening on C_{33}. Note, however, from the scale on Fig. 1(d), that the effect of the transition on C_{33} is very small relative to C_{66} and C_{11} of Figs. 1(a) and 1(b). Thus, we believe that the (small) softening on C_{33} must be attributed to a different origin.

So far, we have deliberately neglected the spin degrees of freedom for clarity. As the ferroelastic and magnetic transitions coincide at T_{N1}, it is clear that spin-lattice interactions need to be considered. Moreover, it is well established[3,10] that the coupling of the magnetic moments with the lattice deformations play a crucial role in the unusual properties of $CuFeO_2$. Considering that the magnetic moments align along the z axis, the lower-order terms consistent with the $R\bar{3}m$ symmetry associated with the spins are

$$F_{es} = \frac{1}{2}A_sS_z^2 + \frac{1}{4}B_sS_z^4 + \beta s_1S_z^2(e_1+e_2) + \beta s_3S_z^2e_3, \quad (12)$$

with $A_s=a_1(T-T_{N1})$. Adding this contribution to the previous total free energy leads to

$$S_z^2 \propto Q_1^2, \quad (13)$$

indicating that both order parameters are coupled. As the softening on C_{66} can only be attributed to Q_1, we conclude that the pseudoproper ferroelastic transition drives the magnetic phase transition at T_{N1}. It is then possible that the softening of C_{33} is simply due to spin fluctuations, while the increase below T_{N2} could be attributed to a biquadratic coupling term between S_z and e_3, as in another typical triangular frustrated antiferromagnet compound, $CsNiCl_3$.[35]

VI. DISCUSSION AND CONCLUSIONS

Through detailed high resolution ultrasonic velocity measurements, symmetry arguments, and the development and analysis of a Landau model free energy, the $R\bar{3}m$-$C2/m$ structural phase transition at 13.7 K in $CuFeO_2$ has been identified as pseudoproper ferroelastic. The proposed model is analogous to the one used for NaN_3. However, while the softening in NaN_3 is associated with an acoustic mode, the analogous softening in $CuFeO_2$ is due to a coupling with an E-symmetric mode (possibly an optical mode which could be Raman active). Strong evidence of this coupling is supported by the nonlinear temperature of the principal elastic constants. Moreover, the large softening observed in C_{66}, with lesser temperature-dependent anomalies in C_{11} and C_{44}, are consistent with this assumption and numerical predictions obtained from the model. Below T_{N1}, the lack of ultrasonic anisotropy in the xy plane is explained by the presence of elastic domains associated with the ferroelastic transition. Thus, our investigation suggests that the crystal structure below T_{N1} is $C2/m$. We believe that the uncertainty in the interpretation of earlier x-ray diffraction results, over the intermediate 3 K region, can be attributed to ferroelastic domains having trigonal symmetry and persisting for a few degrees below 13.7 K.

There is little doubt that the measured elastic properties are strongly affected by the magnetic phase transitions at both temperatures. Our analysis also indicates that while the transition at T_{N1} is ferroelastic in nature, the z component of the spin polarization (S_z) acts as a secondary order parameter. In this scenario, it is possible to account for the elastic and magnetic properties of $CuFeO_2$ above and below T_{N1}. While the model works reasonably well around T_{N1}, it is clear that some of the key elements are still missing in order to account for the lower temperature properties. For example, in order to account for the $R\bar{3}m \rightarrow C2/m \rightarrow \bar{1}$ phase sequence observed in $CuFeO_2$,[10] results presented by Tolédano and Tolédano[36] indicate that the Landau free energy (1) needs to be modified by considering higher-order terms. Moreover, it has been speculated by Terada *et al.*[13,14] that the distortion taking place below T_{N2} is driven by the onset of the period-4 spin structure. An alternate point of view, as in the case of Ho,[8,37] would be to attribute the

stability of the period-4 spin structure to a large magnetoelastic coupling. All these issues will be explored further within the framework of a Landau-type free energy constructed from symmetry arguments which include both spin-spin and spin-lattice coupling.

ACKNOWLEDGMENTS

This work was supported by grants from the Natural Science and Engineering Research Council of Canada (NSERC) as well as from the Canada Foundation for Innovation (CFI).

[1] T. Kimura, T. Goto, H. Shintani, K. Ishizka, T. Arima, and Y. Tokura, Nature (London) **426**, 55 (2003).
[2] G. Lawes *et al.*, Phys. Rev. Lett. **95**, 087205 (2005).
[3] T. Kimura, J. C. Lashley, and A. P. Ramirez, Phys. Rev. B **73**, 220401(R) (2006).
[4] A. B. Harris, Phys. Rev. B **76**, 054447 (2007).
[5] M. Fiebig, J. Phys. D **38**, R123 (2005).
[6] S. Mitsuda, N. Kasahara, T. Uno, and M. Mase, J. Phys. Soc. Jpn. **67**, 4026 (1998).
[7] O. A. Petrenko, G. Balakrishnan, M. R. Lees, D. M. Paul, and A. Hoser, Phys. Rev. B **62**, 8983 (2000).
[8] M. L. Plumer, Phys. Rev. B **76**, 144411 (2007).
[9] F. Ye, Y. Ren, Q. Huang, J. A. Fernandez-Baca, P. Dai, J. W. Lynn, and T. Kimura, Phys. Rev. B **73**, 220404(R) (2006).
[10] N. Terada, Y. Tanaka, Y. Tabata, K. Katsumata, A. Kikkawa, and S. Mitsuda, J. Phys. Soc. Jpn. **75**, 113702 (2006).
[11] H. Takahashi, Y. Motegi, R. Tsuchigane, and M. Hasegawa, J. Magn. Magn. Mater. **272-276**, 216 (2004).
[12] W. M. Xu, M. P. Pasternak, and R. D. Taylor, Phys. Rev. B **69**, 052401 (2004).
[13] N. Terada, S. Mitsuda, H. Ohsumi, and K. Tajima, J. Phys. Soc. Jpn. **75**, 23602 (2006).
[14] N. Terada *et al.*, Phys. Rev. B **75**, 224411 (2007).
[15] T. Kushida and R. W. Terhune, Phys. Rev. B **30**, 3554 (1984).
[16] T. Kushida and R. W. Terhune, Phys. Rev. B **34**, 5791 (1986).
[17] B. Mróz, H. Kiefte, M. J. Clouter, and J. A. Tuszyński, Phys. Rev. B **43**, 641 (1991).
[18] J.-C. Tolédano and P. Tolédano, Phys. Rev. B **21**, 1139 (1980).
[19] E. Dieulesaint and D. Royer, *Elastic Waves in Solids* (Wiley, New York, 1980).
[20] S. Mitsuda, M. Mase, K. Prokes, H. Kitazawa, and H. A. Katori, J. Phys. Soc. Jpn. **69**, 3513 (2000).
[21] P. Tolédano, M. M. Fejer, and B. A. Auld, Phys. Rev. B **27**, 5717 (1983).
[22] G. Quirion, W. Wu, J. Rideout, and B. Mróz, arXiv:cond-mat/0606064 (unpublished).
[23] P. S. Peercy and I. J. Fritz, Phys. Rev. Lett. **32**, 466 (1974).
[24] E. M. Brody and H. Z. Cummins, Phys. Rev. Lett. **21**, 1263 (1968).
[25] G. Errandonea and H. Savary, Phys. Rev. B **24**, 1292 (1981).
[26] A. Pinczuk, G. Burns, and F. H. Dacol, Solid State Commun. **24**, 163 (1977).
[27] H. Hellwig, A. F. Goncharov, E. Gregoryanz, H. K. Mao, and R. J. Hemley, Phys. Rev. B **67**, 174110 (2003).
[28] E. K. H. Salje, *Phase Transitions in Ferroelastic and Co-elastic Crystals* (Cambridge University Press, Cambridge, England, 1990).
[29] M. Tinkhan, *Group Theory and Quantum Mechanics* (Dover, New York, 2003).
[30] A. I. M. Rae, J. Chem. Phys. **70**, 639 (1978).
[31] S. R. Aghdaee and A. I. M. Rae, J. Chem. Phys. **79**, 4558 (1983).
[32] W. Rehwald, Adv. Phys. **22**, 721 (1973).
[33] M. Hasegawa, M. Tanaka, T. Yagi, H. Takei, and A. Inoue, Solid State Commun. **128**, 303 (2003).
[34] D. Sahu, Phys. Rev. B **34**, 4735 (1986).
[35] G. Quirion, T. Taylor, and M. Poirier, Phys. Rev. B **72**, 094403 (2005).
[36] J. C. Tolédano and P. Tolédano, *The Landau Theory of Phase Transitions* (World Scientific, Singapore, 1987), Vol. 3.
[37] M. L. Plumer, Phys. Rev. B **44**, 12376 (1991).